Proceedings of the
Annual Stability Conference
Structural Stability Research Council
Orlando, Florida, April 12-15, 2016

Analysis and Design of Noncompact and Slender Rectangular CFT Columns Subjected to Ambient and Elevated Temperature

Zhichao Lai[1], Amit H. Varma[2], Hua Yang[3] and Anil Agarwal[4]

Abstract
The current AISC Specification (AISC 360-10) specifies the design equations for estimating the axial strength of concrete-filled steel tube (CFT) columns subjected to ambient temperature. However, these equations are over-conservative for noncompact and slender CFT columns, and the effect of elevated temperature on the axial strength is not included. To address these, the authors conducted a two-stage research. In the first stage, the AISC design equations are modified to better predict the axial strength of noncompact and slender CFT columns under ambient temperature, using the effective steel and concrete stress-strain relationships developed and verified by the authors in a previous research. These effective stress-strain relationships implicitly account for the effects of geometric imperfections, steel tube local buckling, steel hoop stresses and concrete confinement. In the second stage, the modified design equations are further improved to include the effects of elevated temperature, using benchmarked heat transfer analysis model and nonlinear inelastic column buckling analysis (NICB) model.

1. Introduction
CFT members consist of rectangular or circular steel tubes filled with concrete. These composite members optimize the use of both steel and concrete construction materials as compared to steel or reinforced concrete structures. The concrete infill delays the local buckling of the steel tube, while the steel tube provides confinement to the concrete infill. The behavior of CFT members under axial loading, flexure, and combined axial and flexural loading can be more efficient than that of structural steel or reinforced concrete members. Moreover, The concrete infill improves the fire resistance (FR) of CFT columns (Hong and Varma 2010).

As an innovative and efficient structural component, CFT members are used widely around the world in various types of structures. In China, CFT members are used in more than three hundred composite bridges. For example, Figure 1(a) shows a typical application of CFT members in a half-through arch bridge. The chords, webs, and bracings of the four-pipe truss are all made of

[1] Ph.D., Postdoctoral research engineer, Purdue University, Lyles School of Civil Eng., West Lafayette, IN. <laiz@purdue.edu>
[2] Professor, Purdue University, Lyles School of Civil Eng., West Lafayette, IN. < ahvarma@purdue.edu >
[3] Professor, Harbin Institute of Technology, School of Civil Eng., Harbin, China < yanghua@hit.edu.cn >
[4] Assistant Professor, Department of Civil Eng., Indian Institute of Technology Hyderabad, Telangana, India, <anil@iith.ac.in>

circular CFTs. CFT members are also used as columns in composite moment or braced frames, for example in: (1) 3 Houston Center in Houston, Texas, (ii) Wuhan International Financial Center in Wuhan, China, and (iii) Taipei 101 tower in Taipei, Taiwan. Figure 1(b) shows a typical application of circular CFT members as mega columns in composite braced frames. CFT members are also used as piles, transmission towers, and bracing members in buckling restrained frames, etc.

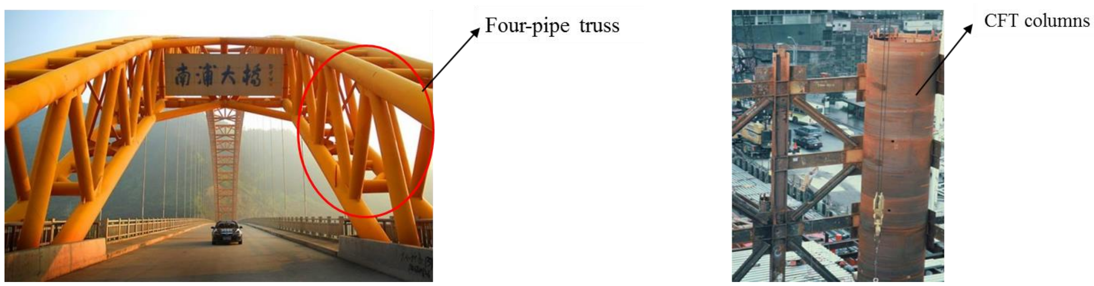

(a) (b)

Figure 1: Typical application of CFT members in: (a) Arch bridges; and (b) Composite braced frames (figure adapted from Lai and Varma 2015).

The current AISC Specification (AISC 360-10) specifies the slenderness limits (λ_p, λ_r, and λ_{limit}, as shown in Table 1) to categorize CFT columns into compact, noncompact or slender depending on the governing slenderness ratio (width-to-thickness *b/t*, λ) of the steel tube. The authors have presented the development of these slenderness limits in detail in Lai et al. (2014) and Lai et al. (2015).

For a CFT columns, if the governing tube slenderness ratio (λ) is less than or equal to λ_p, the member is classified as compact; if the governing tube slenderness ratio is greater than λ_p but less than or equal to λ_r, the member is classified as noncompact; if the governing tube slenderness ratio is greater than λ_r, the member is classified as slender. The tube slenderness ratio is also limited to a maximum permitted value λ_{limit} due to: (i) the lack of experimental data for CFTs with such slender steel tubes, and (ii) potential issues with deflections and stresses in the slender tube walls due to concrete casting pressures and other fabrication processes.

Table 1: Slenderness limits for rectangular CFT columns

Description of Element	Width-to-Thickness Ratio	λ_p Compact/ Noncompact	λ_r Noncompact/Slender	λ_{limit} Maximum Permitted
Steel tube walls of Rectangular CFT Members	*b/t*	$2.26\sqrt{\frac{E_s}{F_y}}$	$3.00\sqrt{\frac{E_s}{F_y}}$	$5.00\sqrt{\frac{E_s}{F_y}}$

2. Background

Since the first documented experimental research on CFT columns by Klöppel and Goder (1957), significant research has been conducted to investigate the behavior of CFT columns. For example, axial compression tests have been conducted by Furlong (1967), Knowles and Park (1969), Anslijin and Janss (1974), Bridge (1976), Lin (1988), Sakino and Hayashi (1991), Bridge and Webb (1993), Bergmann (1994), Fujimoto et al. (1995), Yoshioka et al. (1995), O'Shea and

Bridge (1996), Song and Kwon (1997), Schneider (1998), Han and Yan (2000), Uy (1998, 2001), Kang et al. (2001), Mursi and Uy (2004), and Guo et al. (2007) among others.

Significant research have also been conducted to investigate the fire behavior of CFT columns. For example, standard fire tests have been conducted by Okada et al. (1991), Sakumoto et al. (1994), Lie and Irwin (1995), Kodur and Lie (1996), (Han 2001), Han et al. (2003), and Hong (2007) among others. Numerical models have been developed by Lie (1994), Lie and Stringer (1994), Lie and Irwin (1995), Yin et al. (2006), Hong and Varma (2009), and Hong and Varma (2010) among others. These research indicate that: (1) CFT columns with fire protection have greater FRR values (approximately 120 min) that those without fire protection (approximately 30 min); (2) CFT columns with reinforced concrete infill have greater FRR values (approximately 180 min) that those with plain concrete infill (approximately 120 min).

However, most of these research focus on compact CFT members and the FRR values. This results in the lack of knowledge in: (1) the fundamental behavior of noncompact and slender CFT columns, and (2) the fundamental force-deformation behavior and stability of CFT columns under fire loading. Due to this lack of knowledge, the current AISC Specification (AISC 360-10) uses over-conservative design equations for noncompact and slender CFT columns subjected to ambient temperature, and the effect of elevated temperature on the axial strength is not included.

To address these, a two-stage research was conducted by the authors. In the first stage, the AISC 360-10 design equations are modified using the effective steel and concrete stress-strain relationships developed and verified by the authors in a previous research (Lai and Varma 2016). These effective stress-strain relationships implicitly account for the effects of geometric imperfections, steel tube local buckling, steel hoop stresses and concrete confinement from the transverse interaction between the steel tube and concrete infill. In the second stage, the modified design equations are further improved to include the effects of fire loading, using benchmarked heat transfer (HT) analysis model (developed by Hong and Varma 2010) and nonlinear inelastic column buckling analysis (NICB) model (developed by the authors in Lai et al. 2015 and Lai and Varma 2016). This paper presents: (1) results from the first stage, including the modified design equations and summaries of the effective stress-strain relationship; and (2) representative results of the HT-NICB analysis.

3. Modified AISC 360-10 design equations for ambient temperature

3.1 Evaluation of the AISC 360-10 design equations

AISC 360-10 specifies the design equations to estimate the axial strength of rectangular CFT columns. According to AISC 360-10, the nominal compressive strength (P_{no}) of rectangular CFT sections can be estimated using Eqs. 1-5 as follow.

When the CFT member is compact,

$$P_{no} = P_p = A_s F_y + C_2 f'_c A_c \tag{1}$$

where C_2 is 0.85 for rectangular sections.

When the CFT member is noncompact,

$$P_{no} = P_p - \frac{P_p - P_y}{(\lambda_r - \lambda_p)^2}(\lambda - \lambda_p)^2 \tag{2}$$

where,

$$P_y = A_s F_y + 0.70 f'_c A_c \tag{3}$$

When the CFT member is slender,

$$P_{no} = P_{cr} = A_s F_{cr} + 0.70 f'_c A_c \tag{4}$$

where F_{cr} is the critical buckling stress, which is defined as follows for rectangular sections:

$$F_{cr} = \frac{9E_s}{(b/t)^2} \tag{5}$$

The axial compressive strength (P_n) of rectangular CFT columns can be calculated using Eqs 6-10. In these equations: P_{no} is the nominal compressive strength of the section accounting for tube slenderness using Eqs. 1, 2, or 4; P_e is the elastic (Euler) buckling load of the column calculated using the column length (KL) and effective flexural stiffness (EI_{eff}). The effective flexural stiffness includes contributions of both steel and concrete, and accounts for the effects of concrete cracking.

When $\frac{P_{no}}{P_e} \leq 2.25$ $$P_n = P_{no}[0.658^{\frac{P_{no}}{P_e}}] \tag{6}$$

When $\frac{P_{no}}{P_e} > 2.25$ $$P_n = 0.877 P_e \tag{7}$$

where, $$P_e = \pi^2 \frac{EI_{eff}}{(KL)^2} \tag{8}$$

$$EI_{eff} = E_s I_s + C_3 E_c I_c \text{ E} \tag{9}$$

$$C_3 = 0.6 + [\frac{A_s}{A_c + A_s}] \leq 0.9 \tag{10}$$

The AISC 360-10 design equations (Eqs. 1-10) provide a consistent methodology to estimate the axial compressive strength of rectangular CFT columns under ambient temperature, accounting for length effects, member slenderness, and residual stresses. However, they are over-conservative for noncompact and slender CFT columns, as shown in Figure 2. In this figure, the AISC 36-10 design equations (Eqs. 1-10) were used to predict the strength of 41 test specimens (labeled as "EXP") and 10 columns from additional FEM analyses (labeled as "Additional FEM"). Details of the 41 test specimens are available in the database compiled by the authors for noncompact and slender CFT members (Lai 2014). The additional FEM analyses were conducted by the authors (Lai 2014) to address the gaps in the database.

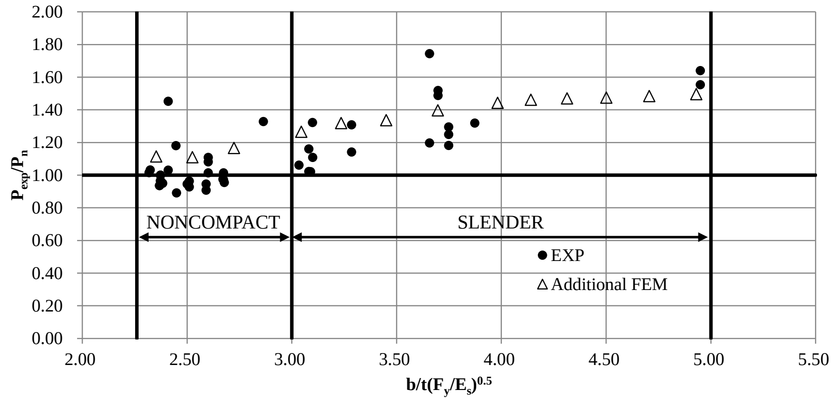

Figure 2: Comparisons of the nominal and experimental strengths for rectangular noncompact and slender CFT columns.

There are two primary reasons for the over-conservatism. The first reason is that the critical buckling stress (F_{cr}) is underestimated by Eq. 5, as shown later in Section 3.2. The second reason is that the effect of concrete confinement is ignored. To address these, more accurate estimation of the critical buckling stress and concrete confinement is required. This is feasible by using the effective-strain relationships developed previously by the authors in Lai and Varma (2016).

3.2 Effective stress-strain relationships

The behavior and strengths of CFT columns and the resulting effective stress-strain relationships depend on several parameters, such as the tube slenderness ratio (b/t), steel yield stress (F_y), and concrete compressive strength (f'_c). In a previous paper (Lai and Varma 2016), the authors have developed the effective-stress strain relationships for steel tube and concrete infill of noncompact and slender CFT members. The effective stress-strain relationships were developed using results from comprehensive parametric studies, which were conducted using FEM models developed and benchmarked previously by the authors in Lai et al. (2014). The FEM models accounted for the effects of geometric imperfections, steel tube local buckling, and steel hoop stresses and concrete confinement from the transverse interaction between the steel tube and concrete infill. Details of the development and verifications of the effective stress-strain relationships have been presented by the authors in Lai and Varma (2016), and are not repeated here for brevity. This section presents the formulation of the developed stress-strain relationships.

For noncompact and slender rectangular CFT columns, the governing failure mode usually involves the local buckling of the steel tube wall, and there is limited confinement provided to the concrete infill. Therefore it is important for the effective stress-strain relationships to model the local buckling stress of the steel tube and limited confinement of the concrete infill.

Figure 3(a) shows the developed effective stress-strain relationship for the steel tube of rectangular CFT columns. As shown, two anchor points (ε_p, σ_p and $2\varepsilon_y$, σ_2) are required to define it: σ_p is the peak stress (i.e., steel critical buckling stress), ε_p is the peak strain (ε_p), ε_y is the steel yield strain, and σ_2 is the post-buckling stress at $2\varepsilon_y$. These anchor points can be calculated using

Eqs. 11-13. Figure 3(b) shows the effective stress-strain relationship for the concrete infill of rectangular CFT columns. The formulation of this relationship is given in Eq. 14, which is the same as the model developed by Popovics (1973). The concrete peak stress (f'_{cp}) can be calculated using Eq. 15.

$$\varepsilon_p = \frac{\sigma_p}{E_s} \tag{11}$$

$$\frac{\sigma_p}{F_y} = 1.12 - 0.11\lambda_{coeff} \le 1.0 \tag{12}$$

$$\frac{\sigma_2}{F_y} = 0.87 - 0.0055\left(\frac{b}{t} - \frac{F_y}{f_c'}\right) \tag{13}$$

$$f_c = f_{cp}' \frac{\varepsilon}{\varepsilon_c} \frac{n}{n-1+\left(\varepsilon/\varepsilon_0\right)^n} \tag{14-a}$$

$$\varepsilon_c = \frac{f_c'}{E_c} \frac{n}{n-1} \tag{14-b}$$

$$n = 0.058 f_c' + 1.0 \tag{14-c}$$

$$\frac{f_{cp}'}{f_c'} = 0.8 + 0.18\left(\frac{b/t}{100} + \frac{F_y/f_c'}{30}\right) \le 1.10 \tag{15}$$

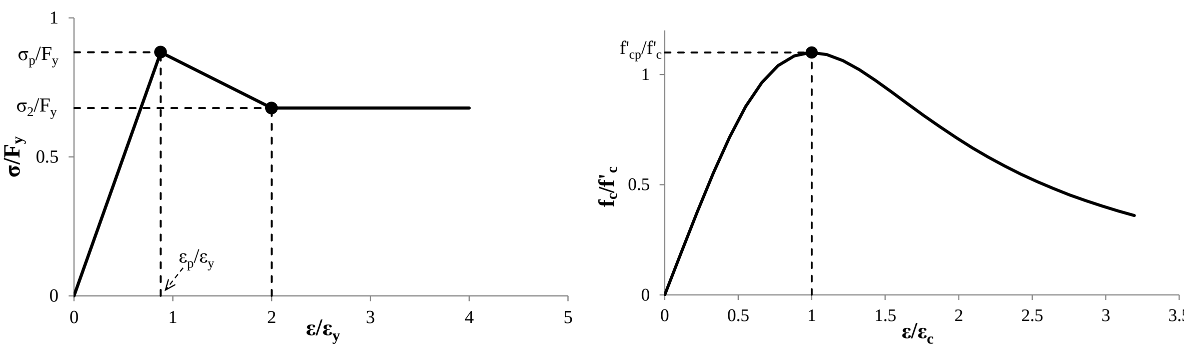

(a) (b)

Figure 3: Idealized effective stress-strain relationship for rectangular CFT members: (a) the steel tube and (b) the concrete infill.

3.3 Proposed design equations for ambient temperature

The nominal compressive strength of CFT section can be calculated using Eq. 16. In this Equation, σ_p can be calculated using Eq. 12, and f'_{cp} can be calculated using Eq. 15.

$$P_{no} = A_s\sigma_p + C_2 f'_{cp} A_c \tag{16}$$

where C_2 is 0.85. This is consistent with the value used for compact CFT columns specified in AISC 360-10.

The axial compressive strength (P_n) of CFT columns can now be calculated using Eqs. 6-10, with P_{no} calculated using Eq. 16. Figure 4 shows the comparisons of the calculated axial strength with the experimental results (data points labeled as "EXP") for all specimens in the database and additional FEM analyses results (data points labeled as "FEM"). The ordinate represents the ratio of experimental-to-calculated value (P_{exp}/P_n), while the abscissa represents the normalized slenderness coefficient (λ_{coeff}). These comparisons indicate that the proposed equations can well predict the axial strength of CFT columns, and reduce the over-conservatism of the AISC 360-10 design equations.

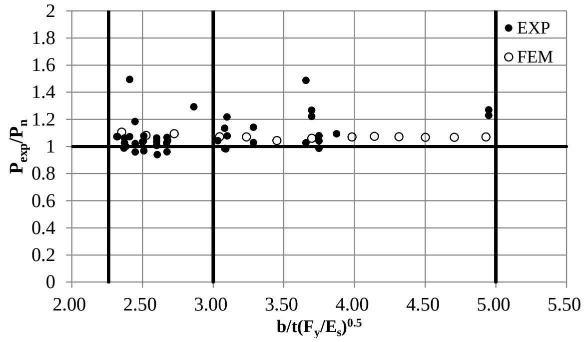

Figure 4: Comparisons of the calculated axial strength with the experimental results and additional FEM analyses results for rectangular CFT columns.

4. Hear transfer (HT)-nonlinear inelastic column buckling (NICB) analysis

As shown in the previous section, the modified AISC design equations (Eqs. 6-10, Eq. 12, Eq. 15, and Eq. 16) can favorably predict the strengths of noncompact and slender CFT columns subjected to ambient temperature. However, the effect of elevated temperature has not been evaluated. To address this, an HT-NICB analysis approach was developed in this section.

The HT-NICB analysis approach consists of two steps, i.e., the two dimensional (2D) heat transfer analysis and the NICB analysis. The first step calculates the temperature distributions of a CFT column cross-section subjected to standard fire loading, and the second step calculates the axial strength (P_n) of a CFT column under temperature distributions calculated from the first step. Both steps were implemented in Matlab (V 2011a).

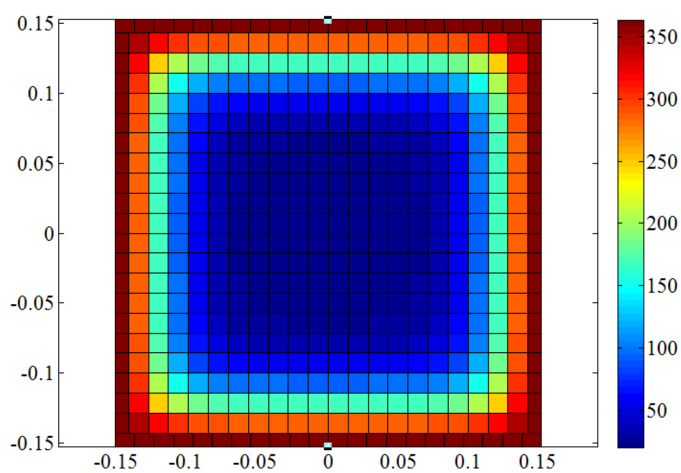

Figure 5: Discretization and temperature distribution (in C°) of CFT cross-section

4.1 2D HT analysis

In standard fire tests, the column specimens were subjected to uniform loading from all sides and along the length (Hong and Varma 2010). Experimental tests indicate that the temperature distributions are: (1) uniform along the length, and (2) approximately double symmetric through the cross-section. Therefore, it is reasonable to use 2D HT analysis of the cross-section to calculate the temperature distribution. In the 2D HT analysis, a CFT cross-section is discretized into layers of fiber, as shown in Figure 5. Figure 5 also shows an example of the temperature distributions of a CFT column (with fire protection) subjected to 20 mins of standard fire loading. Details of development and benchmarking have been presented in Hong and Varma (2010), and not repeated for brevity.

4.2 NICB analysis

The NICB analysis calculates the axial strength (P_n) of a CFT column under temperature distributions calculated from the first step. Algorithm of this analysis approach is shown in Figure 6 and explained in detail as follows. A CFT member was discretized into n-1 (e.g.,14) segments as shown in Figure 7, and the cross section of a CFT member was discretized into layers of fibers as shown in Figure 5. Axial loading was then applied incrementally (and monotonically) to the CFT member until the axial strength (P_{cr}) was reached. For each load increment (P_i,), two analysis subroutines were called consecutively: the $P\!-\!M\!-\!\phi$ subroutine and the Δ subroutine. The $P\!-\!M\!-\!\phi$ subroutine was used to calculate the axial load-moment-curvature ($P\!-\!M\!-\!\phi$) curve using cross-sectional fiber analysis, and the Δ subroutine was used to calculate converged member deflections using corresponding $P\!-\!M\!-\!\phi$ curves. Based on the applied axial load (P_i) and the calculated deflections (Y_k^i), external moments (M_k) including the secondary moments were calculated. The column failure was assumed to occur (i.e., the P_n is reached) when the calculated external moment ($M_k^{i,j}$, see Figure 7) at any station (typically at mid-height) had become greater than the section moment capacity obtained from the $P\!-\!M\!-\!\phi$ subroutine. Other details have been presented by the authors in Lai et al. (2015) and Lai and Varma (2016), and are not discussed here for brevity.

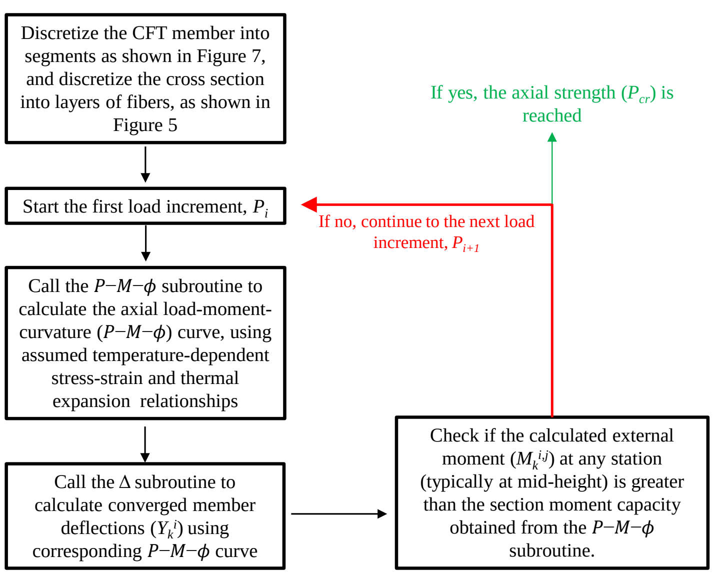

Figure 6: Algorithm of the NICB analysis approach (figure adapted from Lai and Varma 2016)

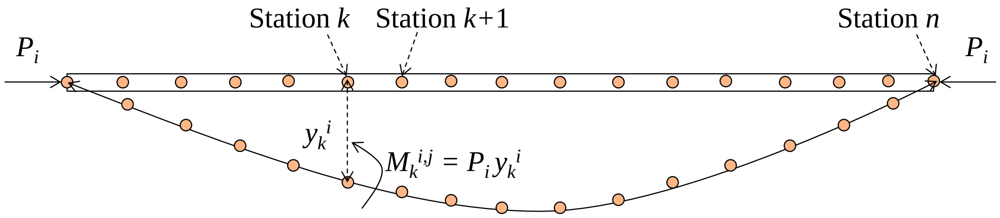

Figure 7: Discretization of the segments along the length (figure adapted from Lai and Varma 2016)

5. Current progress and future work

The HT-NICB analysis approach is currently being used to investigate the axial strength (P_T) of CFT columns under elevated temperature. It is expected that the P_T-P_{no} relationship will be developed for different temperature values. The axial strength of noncompact and slender rectangular CFT columns under elevated temperature can be then estimated using: (1) the modified AISC 360-10 equations, and (2) the P_T-P_{no} relationship.

6. Summary and conclusions

This paper presented the two-stage research conducted to estimate the axial strength of noncompact and slender rectangular CFT columns. In the first stage, the over-conservative AISC 360-10 design equations were modified to better predict the axial strength of noncompact and slender CFT columns under ambient temperature. The modified equation were proposed using the effective steel and concrete stress-strain relationships, which implicitly account for the effects of geometric imperfections, steel tube local buckling, steel hoop stresses and concrete confinement. In the second stage, details of a two-step HT-NICB analysis approach was presented. The HT-NICB analysis approach will be used to develop P_T-P_{no} relationship for noncompact and slender rectangular CFT columns, which can be used to estimate the the axial strength (P_T) of CFT columns under elevated temperature.

References

AISC 360-10. (2010). *Specification for structural steel buildings*. AISC, Chicago, IL, USA.

Bergmann, R. (1994). "Load introduction in composite columns filled with high strength concrete." *Tubular Structures VI, Proceedings of the Sixth International Symposium on Tubular Structures*, P. Grundy, A. Holgate, and B. Wong, eds., Taylor & Francis, Melbourne, Australia, 373–380.

Bridge, R. Q. (1976). "Concrete filled steel tubular columns, Report no. 283, School of Civil Engineering." *Report No. 283, School of Civil Engineering, University of Sydney*, University of Sydney.

Bridge, R. Q., and Webb, J. (1993). "Thin walled circular concrete filled steel tubular columns." *Composite Construction in Steel and Concrete II, Proceedings of the Engineering Foundation Conference*, W. S. Easterling and W. M. Roddis, eds., ASCE, Potosi, Missouri, 634–649.

Fujimoto, T., Nishiyama, I., Mukai, A., and Baba, T. (1995). "Test results of eccentrically loaded short columns -- square CFT columns." *Proceedings of the Second Joint Technical Coordinating Committee Meeting, U.S.-Japan Cooperative Research Program, Phase 5: Composite and Hybrid Structures*, National Science Foundation, Honolulu.

Furlong, R. W. (1967). "Strength of steel-encased concrete beam Columns." *Journal of the Structural Division, ASCE*, 93(ST5), 113–124.

Guo, L., Zhang, S., Kim, W.-J., and Ranzi, G. (2007). "Behavior of square hollow steel tubes and steel tubes filled with concrete." *Thin-Walled Structures*, 45(12), 961–973.

Han, L. H. (2001). "Fire performance of concrete filled steel tubular beam-columns." *Journal of Composites for Construction*, 57(6), 695–709.

Han, L. H., Yang, Y. F., and Xu, L. (2003). "An experimental study and calculation on the fire resistance of concrete-filled SHS and RHS columns." *Journal of Constructional Steel Research*, 59(4), 427–452.

Han, L.-H., and Yan, S. . (2000). "Experimental studies on the strength with high slenderness ratio concrete filled steel tubular columns." *Proceedings of the Sixth ASCCS International Conference on Steel-Concrete Composite Structures*, Y. Xiao and S. . Mahin, eds., Association for International Cooperation and Research in Steel-Concrete Composite Structures, Los Angeles, 419–426.

Hong, S. (2007). "Fundamental behaviour and stability of CFT columns under fire loading [Dissertation]." Purdue University.

Hong, S., and Varma, A. H. (2009). "Analytical modeling of the standard fire behavior of loaded CFT columns." *Journal of Constructional Steel Research*, Elsevier Ltd, 65(1), 54–69.

Hong, S., and Varma, A. H. (2010). "Predicting fire behavior of composite CFT columns using fundamental section behavior." *Journal of ASTM International*, 7(1), 78–110.

Janss, J., and Anslijn, R. (1974). "Le Calcul des Charges Ultimes des Colonnes Métalliques Enrobés de Béton." *Rapport CRIF*, *MT*, 89, (Bélgica).

Kang, C. H., Oh, Y. S., and Moon, T. S. (2001). "Strength of axially loaded concrete-filled tubular stub column." *International Journal of Steel Structures*, 13(3), 279–287.

Klöppel, K., and Goder, W. (1957). "Traglastversuche mit ausbetonierten Stahlrohen und Aufstellung einer Bemessungsformel." *Der Stahlbau, Berlin*, 26(1).

Knowles, R. B., and Park, R. (1969). "Strength of concrete filled steel tubular columns." *Journal of the Structural Division, ASCE*, 95(ST12), 2565–2587.

Kodur, V. K. R., and Lie, T. T. (1996). "Fire Resistance of Circular Steel Columns Filled With Fiber-Reinforced Concrete." *Journal of Structural Engineering*, 122(7), 776–782.

Lai, Z. (2014). "Experimental database, analysis and design of noncompact and slender concrete-filled steel tube (CFT) members [Dissertation]." Purdue University.

Lai, Z., and Varma, A. H. (2015). "Noncompact and slender circular CFT members: experimental database, analysis, and design." *Journal of Constructional Steel Research*, 106(3), 220–233.

Lai, Z., and Varma, A. H. (2016). "Effective stress-strain relationships for noncompact and slender CFT members." *Engineering Structures (Revision submitted)*.

Lai, Z., Varma, A. H., and Connor, R. J. (2015). "Retrofit of built-up steel columns: modeling and fundamental behavior." *Journal of Bridge Engineering*.

Lai, Z., Varma, A. H., and Griffis, L. G. (2015). "Analysis and design of noncompact and slender CFT beam-columns." *Journal of Structural Engineering*.

Lai, Z., Varma, A. H., and Zhang, K. (2014). "Noncompact and slender rectangular CFT members: Experimental database, analysis, and design." *Journal of Constructional Steel Research*, 101, 455–468.

Lie, T. ., and Irwin, R. J. (1995). "Fire resistance of rectnagular steel columns filled with bar-reinforced concrete." *Journal of Structural Engineering*, 121(May 2011), 797–805.

Lie, T. T. (1994). "Fire resistance of circular steel columns filled with bar-reinforced concrete." *Journal of Structural Engineering*, 120(5), 1489–1509.

Lie, T. T., and Stringer, D. C. (1994). "Calculation of fire resistance of steel hollow structural steel columns filled with plain concrete." *Canadian Journal of Civil Engineering*, 21(3), 382–385.

Lin, C. Y. (1988). "Axial capacity of concrete infilled cold-formed steel columns." *Ninth International Specialty Conference on Cold-Formed Steel Structures*, W.-W. Yu and H. S. Joseph, eds., University of Missouri - Rolla, St. Louis, 443–457.

Mursi, M., and Uy, B. (2004). "Strength of slender concrete filled high strength steel box columns." *Journal of Constructional Steel Research*, 60(12), 1825–1848.

O'Shea, M. D., and Bridge, R. Q. (1996). "Circular thin-walled tubes with high strength concrete." *Composite Construction in Steel and Concrete III, Proceedings of the Engineering Foundation Conference*, C. D. Buckner and B. M. Shahrooz, eds., American Society of Civil Engineers, Irsee, Germany, 780–793.

Okada, T., Yamaguchi, T., and Sakumoto, Y. (1991). "Load heat tests of full-scale columns of concretefilled tubular steel structure using fire-resistant steel for buildings." *Third International Conference on Steel–Concrete Composite Structures*, ASCCS, Fukuoka, 101–106.

Popovics, S. (1973). "A numerical approach to the complete stress-strain curve of concrete." *Cement and Concrete Research*, 3, 583–599.

Sakino, K., and Hayashi, H. (1991). "Behavior of concrete filled steel tubular stub columns under concentric loading." *Proceedings of the Third International Conference on Steel-Concrete Composite Structures*, M. Wakabayashi, ed., Association for International Cooperation and Research in Steel-Concrete Composite Structures, Fukuoka, Japan, 25–30.

Sakumoto, Y., Okada, T., Yoshida, M., and Tasaka, S. (1994). "Fire resistance of concrete-filled, fire-resistant steel-tube columns." *Journal of Materials in Civil Engineering*, 6(2), 169–184.

Schneider, S. P. (1998). “Axially loaded concrete-filled steel tubes.” *Journal of Structural Engineering*, 124(October), 1125–1138.

Song, J. Y., and Kwon, Y. . (1997). “Structural behavior of concrete-filled steel box.” *Composite Construction-Conventional and Innovative, International Conference*, International Association for Bridge and Structural Engineering, Innsbruck, Austria, 795–800.

Uy, B. (1998). “Local and post-local buckling of concrete filled steel welded box columns.” *Journal of Constructional Steel Researchournal of Constructional Steel Research*, 47, 47–72.

Uy, B. (2001). “Strength of short concrete filled high strength steel box columns.” *Journal of Constructional Steel Research*, 57(2), 113–134.

Yin, J., Zha, X., and Li, L. (2006). “Fire resistance of axially loaded concrete filled steel tube columns.” *Journal of Constructional Steel Research*, 62(7), 723–729.

Yoshioka, K., Inai, E., Hukumoto, N., Kai, M., Murata, Y., Noguchi, T., Tanaka, Y., Tokinoya, H., and Mukai, A. (1995). “Compressive tests on CFT short columns. Part 1: Circular CFT columns.” *Proceedings of the Second Joint Technical Coordinating Committee (JTCC) on Composite and Hybird Structures, Phase 5: Composite and Hybrid Structures*, National Science Foundation, Honolulu,Hawaii.